

Performance analysis of plate-fin heat exchanger used for case drain oil cooling application in variable displacement pumps

Karthik S Ramachandra¹, S S Manjunatha², K N Seetharamu³

¹Department of Mechanical Engineering, B N M Institute of Technology, Bengaluru

²Pascal Systemtechnik pvt. ltd., Bengaluru

³Department of Mechanical Engineering, P E S University, Bengaluru

E-mail: srkarthikvinu@gmail.com

Abstract. Variable displacement pumps are commonly employed in fluid power equipment. In applications involving variable displacement pumps, overheating of oil is a frequently encountered problem necessitating an effective oil cooling solution. In this work, the thermo-hydraulic performance analysis of an air blast hydraulic oil cooler, which is a compact heat exchanger (Brazed Aluminium Plate-Fin type) with surface heat enhancement feature in the form of rectangular offset strip fins is presented. The performance models available in the literature present correlations for f and j factors limited to a particular surface geometry and Reynolds number Re range. In the present work a detailed theoretical thermo-hydraulic analysis of an existing heat exchanger is presented using models available in the literature and also experimentally validated using a developed test-rig. The performance parameters derived from f and j factors like exchanger effectiveness, heat transfer coefficients and pressure drop are amply addressed. It was found that, cooler effectiveness varied only slightly with increasing oil inlet temperatures; whereas effectiveness decreased with increasing flow rates. The heat transfer rates increased with increasing oil flow rates and also with increasing oil inlet temperatures. The pressure drop on the oil side was found negligible.

1. Introduction

Hydraulic pumps form an integral part of almost all hydraulic systems. In a variable displacement pump, pumping chamber sizes can be changed using displacement control, changing the drive speed, or doing both; resulting in changing delivery from the pump. These pumps are used in a closed center system [i.e.the pump continues to operate against a load in the neutral condition]. Overheating is one of the commonly encountered problems in hydraulic equipment. Though there are many reasons for heat generation in hydraulic components and systems, the inefficiency of the pump and friction in the pipes, joints, line fittings etc. are the major contributors for heat generation. Air cooled compact heat exchangers are commonly employed to address the problem of overheating. A gas-to-fluid compact heat typically has a heat transfer surface with a surface area to volume ratio of greater than $700\text{ m}^2/\text{m}^3$ on at least one of the fluid sides.



1.1. Location of oil cooler

Not only the type of exchanger but the location of heat exchanger plays an important role in ascertaining the effectiveness of the heat exchanger (cooler). It can be easily recognized that, of all the parameters leading to heating; the contribution of pump is dominant. Also, when variable displacement pumps are used in a closed center system, there is pumping operation even during neutral loads. Continued operation under neutral load thereby results in an increased oil temperature. Now, if the cooler is placed in the return line of the hydraulic circuit, the hot oil inevitably flows through the entire circuit before being cooled resulting in heat related problems in the system as previously quoted. Also, since the temperature of oil in the return line is lower than the maximum temperature reached, a larger heat exchanger is required to obtain necessary temperature difference.

Now, in view of the above drawbacks, a viable option would be to place the cooler in the case drain line of pump. The leakage from the pump flows back to the reservoir through the case drain line. It is obvious that the oil flowing through the case drain will be at a higher temperature compared to oil temperature in the return line. Now, if the case drain flow is used, it enables the use of a smaller and compact heat exchanger, also the oil flow rate in the case drain is lower compared to the return line, resulting in lower pressure drop across the cooler. Even though the flow rate is lower in the case drain line, the reduction in temperature of oil is sufficient enough to maintain a safer operating temperature level.

2. Literature Review

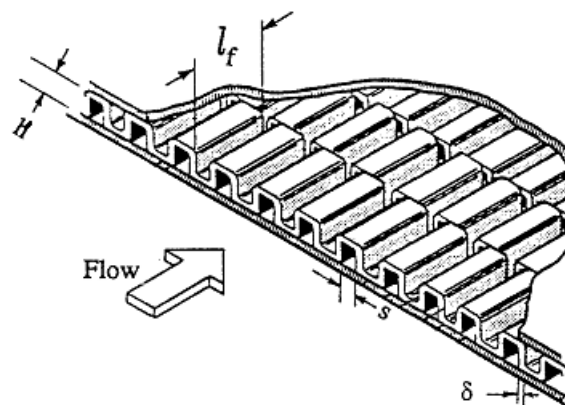
The heat transfer and pressure drop characteristics of a heat exchanger are conveniently expressed in terms of the Colburn factor and Fanning factor respectively. Numerous researchers have carried quality research on the prediction of j and f factors for a wide variety of compact heat exchangers with various fin configurations. Since, the present work is concerned with offset strip fin surfaced plate-fin heat exchangers, literature on the same are reviewed. Kays and London [1] have presented a comprehensive collection of j and f factors vs. Re for a large number of extended surfaces. 33 plate-fin surfaces are reported in the collection. The analytical model considered in the present work for prediction of j and f factors is attributed to Joshi and Webb[2]. This model represents correct behaviour for very small and very large values of Re . There are many empirical correlations available from the literature. Here correlations developed by Wieting [3], Manglik and Bergles [4] for $200 < Re < 10000$ are considered. The correlations developed by Manglik and Bergles are reported to be accurate in all regimes of Re . Experimental investigations were conducted by Michna et.al [5] on the effect of increasing Reynolds number on the performance of offset strip fins. They report an increase in both measured pressure drop and heat transfer coefficients by approximately twice than that predicted by the best available correlation developed using data from low Reynolds number conditions. An investigation on the flow pattern and turbulence intensity in offset strip fin, slotted fin and plain straight fin arrays were performed by Mochizuki et.al [6]. The study conducted was experimental drawing the following conclusion that, the offset strip fin core has higher turbulence intensity and consequently would result in higher heat transfer performance than the slotted fin and plain strip fin cores, mainly due to secondary laminar flow enhancement mechanism. Also, for offset strip fin core with short fins, static pressure falls almost linearly along the flow. A number of numerical studies are also reported in the literature.

3. Theoretical thermo-hydraulic analysis

The analysis part can be broadly classified into a sizing problem and a rating problem. Since the heat exchanger is already sized, only the rating part of the problem was addressed. The steps involved in a rating problem are as follows;

Table 1. Description of the oil cooler

Particulars	
Heat exchanger type	Compact plate-fin type
Material	Aluminum alloy
Working fluids	Hot fluid - hydraulic oil Cold fluid - Air
Flow arrangement	Unmixed cross flow
No. of hot fluid streams	10
No. of cold fluid streams	11
Type of fin arrangement	Offset-strip fin
Depth of Cold stream passage	10.3 mm
Depth of Hot stream passage	2.5 mm
Length of Cold stream passage	32 mm
Length of Hot stream passage	165 mm
Plate thickness	0.8 mm

**Figure 1.** Description of an offset strip fin array

- Surface geometrical characteristic determination: This includes determination of heat transfer surface area (both primary and secondary), the minimum free-flow area, flow lengths, hydraulic diameter, heat transfer surface area density, the ratio of minimum free-flow area to frontal area, fin length, and fin thickness for fin efficiency determination, and any specialized dimensions used for heat transfer and pressure drop correlations.
- Heat transfer calculation: Involves estimation of j factor, heat transfer coefficients, heat dissipation, exchanger effectiveness, etc.
- Pressure drop calculation: Estimating pressure drop on both fluid sides.

3.1. Geometrical characteristics

The oil cooler used in the present study is a compact offset strip fin type, plate fin heat exchanger. The fins provided are rectangular in shape. Fins are provided on both hot and cold fluid sides. The air is forced on to the oil cooler using an axial fan. The details of the fins on cold stream and hot stream side are presented below. The maximum operating pressure for the exchanger

Table 2. Particulars of fins on air side (cold stream) and oil side (hot stream)

Particulars	(cold side - Fluid 1) in mm	(hot side - Fluid 2) in mm
Width of fin, s	2.4	1.2
Length of fin, l_f	8	5
Thickness of fins, δ	0.3	0.03
Depth, H	10.3	2.5
No. of rows of fins	4 rows	33 rows

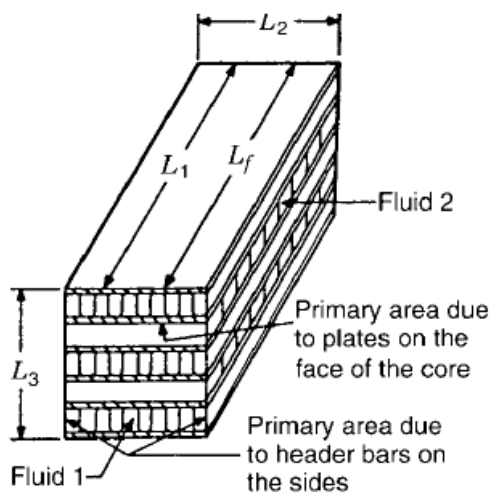
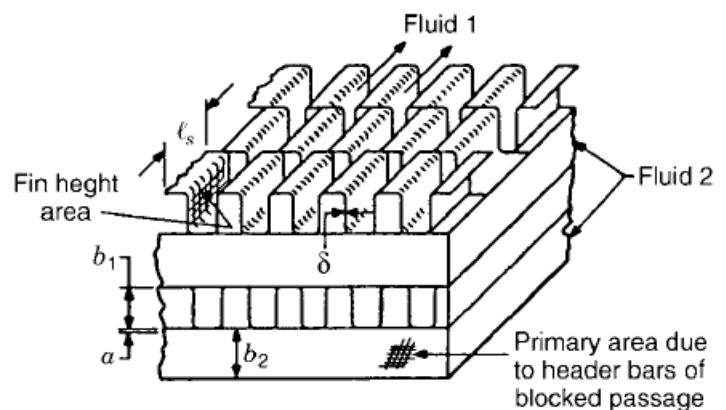
is 5 kg/cm^2 , maximum flow rate is 8 LPM and port size is G1/2. The axial fan used has a rating of 45 W , at 2800 rpm and a flow rate of $325 - 380 \text{ m}^3/\text{h}$. The hydraulic oil used is of ISO grade:68 ($\rho = 886 \text{ kg/m}^3$).

3.1.1. Air side calculation The total heat transfer area consists of primary and secondary surface area swept by the fluid 1 (AIR). The components of the primary surface area are:

- (i) The plate area
- (ii) The fin base area that covers the plate
- (iii) The header bar area on the sides for fluid 1 near the ends of fins in the L_2 direction.
- (iv) Header bars and plates exposed area of the blocked fluid 2 [OIL] passages at fluid 1 core inlet and outlet faces.

The secondary (fin) area consists of;

- (i) The fin height area
- (ii) Fin edge height area
- (iii) Fin edge width area

**Figure 2.** Plate fin heat exchanger**Figure 3.** Offset strip fin geometry

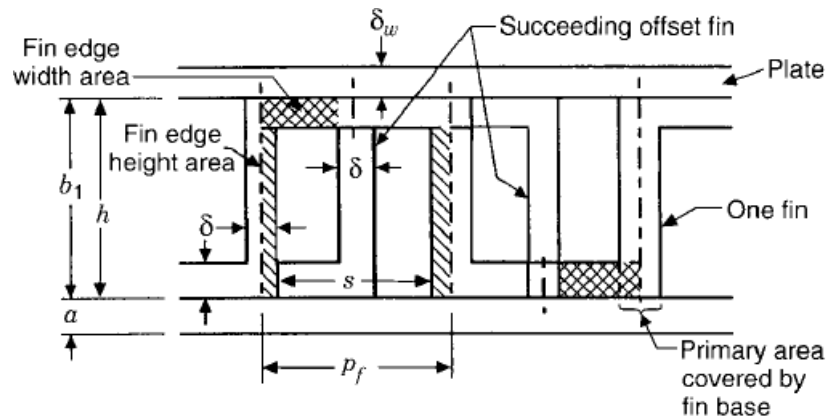


Figure 4. Small section of an idealized offset strip fin geometry

By geometric inspection the primary surface area is obtained as the sum of primary area components i, iii, and iv minus component ii.

Total primary surface area for AIR side,

$$\begin{aligned} A_{(p,1)} &= (i) - (ii) + (iii) + (iv) \\ &= (2L_1L_2N_p) - (2\delta L_F n_f) + (2b_1L_1N_p) + (2(b_2 + 2\delta_w)(N_p - 1)L_2) \\ &= 0.121125m^2 \end{aligned}$$

Total secondary area for AIR side,

$$\begin{aligned} A_{(f,1)} &= (i) + (ii) + (iii) \\ &= (2(b_1 - \delta)L_f n_f) + (2(b_1 - \delta)\delta n_{off} n_f) + ((p_f - \delta)\delta(n_{off} - 1)n_f) + (2p_f n_f \delta) \\ &= 0.440738 m^2 \end{aligned}$$

So, total surface area on the AIR side;

$$A_1 = A_{(p,1)} + A_{(f,1)} = 0.561863 m^2$$

The free-flow area on AIR side is given by the frontal area on AIR side minus the area blocked by the fins at the entrance of the core on that side.

$$A_{(o,1)} = (b_1L_2N_p) - [(b_1 - \delta) + p_f]\delta n_f = 0.015726 m^2$$

Other geometrical characteristics of interest are;

$$\begin{aligned} A_{fr} &= L_2(L_3) = L_2[(N_p - 1)b_2 + N_p b_1 + 2N_p \delta_w] = 0.025116 m^2 \\ \sigma &= \frac{A_{(o,1)}}{A_{fr}} = 0.626 \\ \beta &= \frac{A_1}{V_p} = \frac{A_1}{b_1 N_p L_2 L_1} = 962.55 m^2/m^3 \\ D_h &= \frac{4L_1 A_{(o,1)}}{A_1} = 3.5825 mm \end{aligned}$$

The flow length for ΔP calculation = L_1 .

3.1.2. *Oil side calculation* Repeating the above geometric calculation for fluid 2 (OIL) side, the following results are obtained. Total primary surface area for OIL side,

$$\begin{aligned} A_{(p,2)} &= (i) - (ii) + (iii) + (iv) \\ &= (2L_1L_2N_p) - (2\delta L_F n_f) + (2b_1L_1N_p) + (2(b_2 + 2\delta_w)(N_p + 1)L_2) \\ &= 0.061472m^2 \end{aligned}$$

Total secondary area for OIL side,

$$\begin{aligned} A_{(f,2)} &= (i) + (ii) + (iii) \\ &= (2(b_1 - \delta)L_f n_f) + (2(b_1 - \delta)\delta n_{off} n_f) + ((p_f - \delta)\delta(n_{off} - 1)n_f) + (2p_f n_f \delta) \\ &= 0.086129 m^2 \end{aligned}$$

So, total surface area on the OIL side;

$$A_1 = A_{(p,2)} + A_{(f,2)} = 0.147601 m^2$$

The free-flow area on OIL side is given by the frontal area on OIL side minus the area blocked by the fins at the entrance of the core on that side.

$$A_{(o,2)} = (b_1L_2N_p) - [(b_1 - \delta) + p_f]\delta n_f = 325 mm^2$$

Other geometrical characteristics of interest;

$$\begin{aligned} A_{fr} &= L_2(L_3) = L_2[(N_p + 1)b_2 + N_p b_1 + 2N_p \delta_w] = 0.002777 m^2 \\ \sigma &= \frac{A_{(o,2)}}{A_{fr}} = 0.117 \\ \beta &= \frac{A_2}{V_p} = \frac{A_2}{b_1 N_p L_2 L_1} = 1987.89 m^2/m^3 \\ D_h &= \frac{4L_1 A_{(o,2)}}{A_2} = 1.4532 mm \end{aligned}$$

3.2. Heat transfer calculation

Heat transfer calculation is one of the important steps in the analysis of a heat exchanger. The assumptions for the entire heat transfer analysis and different analysis approaches are listed.

- Steady-state operating conditions.
- Negligible heat losses to surroundings.
- Uniform wall thermal resistance.
- Longitudinal heat conduction is negligible.
- The individual and overall heat transfer coefficients are constant.
- Constant fluid properties at a given temperature.
- Uniform heat transfer surface area on each fluid side.
- Uniform temperature and velocity distribution at the entrance on each fluid side over the flow cross section. There is no gross flow maldistribution at the inlet.
- Heat exchanger wall thermal resistance is assumed uniform and negligible.
- Fouling factor for both fluid sides are assumed negligible.

3.2.1. *Thermal analysis - (ϵ - NTU) method* The procedure employed for heat transfer related calculations are described as follows:

Step 1

To compute the fluid bulk mean temperature and fluid thermo physical properties on each fluid side. Since the outlet temperatures were unknown, they were estimated initially by a reasonable assumption for exchanger effectiveness. For the assumed effectiveness, the fluid outlet temperatures were calculated using,

$$T_{(h,o)} = T_{(h,i)} - \epsilon \frac{C_{min}}{C_h} (T_{(h,i)} - T_{(c,i)})$$

$$T_{(c,o)} = T_{(c,i)} - \epsilon \frac{C_{min}}{C_h} (T_{(h,i)} - T_{(c,i)})$$

where subscripts h and c represent hot and cold fluid respectively.

Assuming, $C_{min}/C_{max} = [(\dot{m}c_p)_{min}]/[(\dot{m}c_p)_{max}]$ with approximate values for specific heat c_p of fluids.

For, AIR initially c_p was assumed as = 1005 J/kgK

For, OIL initially c_p was assumed as = 1950 J/kgK

The fluid bulk mean temperatures were obtained when $C_{min}/C_{max} > 0.5$; for the C_{max} side it is the arithmetic mean of inlet and outlet temperatures; the bulk mean temperature on the C_{min} side is the log mean average temperature which was obtained as follows,

$$T_{C_{(min,m)}} = T_{C_{(max,m)}} \pm \Delta T_{lm}$$

$$LMTD = \Delta T_{lm} = ((T_{(h,i)} - T_{(c,o)}) - (T_{(h,o)} - T_{(c,i)})) / \log \left(\frac{T_{(h,i)} - T_{(c,o)}}{T_{(h,o)} - T_{(c,i)}} \right)$$

The fluid properties that are to be determined at the bulk mean temperature are dynamic viscosity μ , specific heat at constant pressure c_p , Prandtl number Pr and thermal conductivity k .

For AIR;

Fluid properties were determined using correlations relating properties to absolute temperature T ;

$$\rho(T) = 1E^{-6}T^2 - 9.963E^{-3}T + 3.277$$

$$\mu(T) = -4E^{-11}T^2 + 7085.20E^{-11}T + 86421.31E^{-11}$$

$$k(T) = -5E^{-8}T^2 + 10731.5E^{-8}T - 148254.6125E^{-8}$$

$$c_p = 4E^{-4}T^2 - 0.20222T + 1031$$

$$Pr = (\mu c_p)/k$$

For OIL;

From standard properties of Hydraulic Oil ISO 68 at 15 deg C = 886 kgm³

Density at any temperature $t^\circ C$ can be obtained by; $(886(15 + 273.15))/(t + 273.15)$

Kinematic Viscosity $\nu mm^2/s$ for Oil at a given temperature $t^\circ C$ can be determined by using a correlation obtained by curve fitting of Kinematic viscosity vs Temperature graph for ISO 68.

$\nu = 677.02110390 - 37.18097042t + 0.86473485t^2 - 0.00954040t^3 + 0.00004091t^4$ Dynamic Viscosity, $\mu = \rho \nu E^{-6} Ns/m^2$

To calculate specific heat, empirical correlation for petroleum based oil is used [7],

$c_p = ((0.388 + 0.00045t))/\sqrt{d}$ where, c_p is in BTU/lb^oF, d is specific gravity of oil, t is temperature in ^oF. The conversion factor to SI units is 4186.80.

For thermal conductivity, again empirical relation is used [7];

$k = 0.813[1 - 0.0003(t - 32)]/d$ where, k is in $(BTU\ inch)/(ft^2\ hr\ ^\circ F)$. The conversion factor to SI units is 0.144228.

Step 2

Reynolds number; $Re = (\dot{m}D_h)/(\rho A_o)$.

There are various correlations for computing f and j factors for an offset strip fin heat exchanger surfaces. The following correlation by Manglik and Bergles [4] was used in calculation of f and j factors;

Laminar $Re_{D_h} \leq Re_{D_h}^*$

$$\begin{aligned} f &= 9.624(s/H)^{-0.186}(t/L_f)^{0.305}(t/s)^{-0.266} Re_{D_h}^{-0.742} \\ j &= 0.652(s/H)^{-0.154}(t/L_f)^{0.15}(t/s)^{-0.068} Re_{D_h}^{-0.540} \end{aligned}$$

Turbulent $Re_{D_h} \geq (Re_{D_h}^* + 1000)$

$$\begin{aligned} f &= 1.870(s/H)^{-0.094}(t/L_f)^{0.682}(t/s)^{-0.242} Re_{D_h}^{-0.299} \\ j &= 0.244(s/H)^{-0.104}(t/L_f)^{0.196}(t/s)^{-0.173} Re_{D_h}^{-0.406} \end{aligned}$$

Critical Reynolds number;

$$Re_{D_h}^* = (L_f/s)^{1.23}(t/L_f)^{0.58} \left(D_h / \left(t + 1.328(L_f/\sqrt{Re_{L_f}}) \right) \right)$$

The hydraulic diameter was estimated using;

$$D_h = (4sHL_f) / (2(sL_f + HL_f + tH) + ts)$$

The corrected Nusselt number Nu or j and f factor values were obtained by incorporating variable fluid property effects, i.e.

For OIL;

$$\begin{aligned} \frac{Nu}{Nu_{cp}} &= \frac{h}{h_{cp}} = \frac{\mu_w^n}{\mu_m} \\ n &= -0.14 \\ \frac{f}{f_{cp}} &= \frac{\mu_w^m}{\mu_m} \\ m &= 0.54 \end{aligned}$$

For AIR;

$$\begin{aligned} \frac{Nu}{Nu_{cp}} &= \frac{h}{h_{cp}} = \frac{T_w^n}{T_m} \\ n &= 0 \\ \frac{f}{f_{cp}} &= \frac{T_w^m}{T_m} \\ m &= 0 \end{aligned}$$

Step 3

From j the heat transfer coefficients for both the fluids were computed using the relation,

$$h = \frac{j c_p G}{Pr^{2/3}}$$

Fin efficiency η_f was then determined and also the extended surface efficiency η_o was computed as follows;

For an offset strip fin configuration, if it is assumed that the heat flow from both sides (plates) is uniform and the adiabatic plane occurs at the middle of the plate spacing. Hence,

$$l = (b/2) - \delta$$

The perimeter of fin at its cross section is $(2l_s + 2\delta)$ and the cross section is $l_s\delta$.

$$\begin{aligned} ml &= [(1 + (\delta/l_s))2(h/(k_f\delta))]^{0.5} ((b/2) - \delta) \\ \eta_f &= \tanh(ml)/ml \end{aligned}$$

Overall extended surface efficiency;

$$\eta_o = [1 - (1 - \eta_f)(A_f/A)]$$

The wall thermal resistance is calculated using;

$$\begin{aligned} R_w &= \delta_w/(k_w A_w) \\ A_w &= 2L_1 L_2 N_p \end{aligned}$$

Finally to determine UA , neglecting fouling;

$$\frac{1}{UA} = \frac{1}{\eta_o h A}_2 + R_w + \frac{1}{\eta_o h A}_1$$

Subscripts 1 and 2 indicate AIR and OIL respectively.

Step 4

Now, from the known heat capacity rates on each fluid side, C^* is computed. From the known UA , NTU was determined for this case as,

$$NTU = UA/C_{min} = UA/C_c$$

The longitudinal conduction parameter was neglected. The effectiveness of the heat exchanger was then computed using the NTU from the following equation.

For unmixed – unmixed single pass cross flow heat exchanger,

$$\epsilon = 1 - \exp[(\exp(-NTUC^*n) - 1)/(C^*n)]$$

where C^* is the heat capacity ratio and $n = NTU^{-0.22}$

Step 5

With effectiveness value known, the outlet temperatures were calculated using the equations employed in *Step 1*.

If the outlet temperature obtained were found significantly different from the values assumed initially, steps 1 to 5 were repeated using newly obtained outlet temperatures until the assumed and computed outlet temperatures converged within the desired degree of accuracy, which was assumed to be $\Delta = 10^{-06}$.

Step 6

Finally, heat transfer rate was estimated using, $q = \epsilon C_{min}(T_{h,i} - T_{c,i})$

3.3. Pressure drop calculation

The importance of pressure drop calculation is emphasized with the following factors:

- (i) The pumping power essential to pump fluid through the exchanger is proportional to the pressure drop across the exchanger.

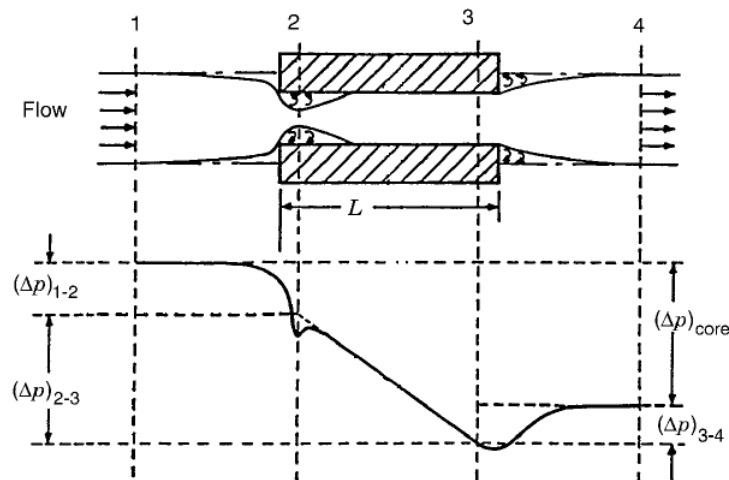


Figure 5. Pressure drop for a small section of an idealized offset strip fin geometry

- (ii) The heat transfer can be influenced significantly by pressure drop (when fluid undergoes change of phase)

The following are the major assumptions for pressure drop analysis:

- (i) Steady state operating conditions.
- (ii) Constant fluid properties at a given temperature.
- (iii) Constant friction factor.

3.3.1. Pressure drop for an offset strip fin surface The components associated with the total pressure drop for an offset strip fin surface are:

- $\Delta p_{1,2}$ is the pressure drop at core entrance due to sudden contraction.
- $\Delta p_{2,3}$ is the pressure drop within the core.
- $\Delta p_{3,4}$ is the pressure rise at the core exit.

The largest contribution to total pressure drop is usually due to $\Delta p_{2,3}$.

The total core pressure drop is given by;

$$\begin{aligned} \Delta p &= \Delta p_{1,2} + (\Delta p_{2,3} - \Delta p_{3,4}) \\ &= \frac{G^2}{(2\rho_o p_i g_e)} \left[(1 - \sigma^2 + K_c) + 2\left(\frac{\rho_i}{\rho_o} - 1\right) + f(L/r_h)\rho_i 1/\rho_m - (1 - \sigma^2 - K_e)\left(\frac{\rho_i}{\rho_o}\right) \right] \\ &= \text{Entrance} + \text{Momentum} + \text{Core friction} + \text{Exit} \end{aligned}$$

The values of K_e and K_c are usually determined from graphs. For highly interrupted fin geometries like offset strip fins, the entrance and exit losses are generally small compared to a high value of the core pressure drop, and the flow is mixed very well. To eliminate use of graphs; expressions for K_c and K_e were derived using curve fitting technique. The equations obtained were as follows:

$$\begin{aligned} K_c &= 0.40461538 + 0.00817016 \sigma - 0.41317016 \sigma^2 \\ K_e &= 0.99895105 - 1.96088578 \sigma + 0.96270396 \sigma^2 \end{aligned}$$

3.3.2. Procedure adopted for pressure drop calculation For the pressure drop calculations, the fluid densities were determined at the exchanger inlet and outlet for each fluid. The mean specific volume was then estimated on each fluid side. Further, the entrance and exit loss coefficients, were obtained for known values, Re , and the flow σ passage entrance geometry.

The friction factors were then obtained using the correlation mentioned. The obtained friction factor on each fluid side was corrected for variable fluid properties.

Wall temperature is given by,

$$T_w = \frac{\left(T_{2m} + \frac{R_2}{R_1}T_{1m}\right)}{1 + \frac{R_1}{R_2}}$$

where R is the thermal resistance. The total pressure drops for both fluid sides are then calculated.

3.4. Programming

The procedure adopted for heat transfer and pressure drop calculations were adapted to a program developed using BASIC programming language. The program conducts multiple trials before giving results for heat transfer and pressure drop.

4. Experimental analysis

To test the heat exchanger a test rig was developed. The test rig designed consists basically of a hydraulic power pack, a flow control valve assembly, a testing block with arrangements for temperature and pressure measurement.

The oil from the oil tank (1) is pumped through the circuit using a gear pump (9) driven using an electric motor (12) via a flexible drive coupling (10). The oil cooler is placed on a specially designed block taking the geometric features of the cooler into consideration. The block has arrangements for mounting temperature sensors for oil temperature measurement both at inlet and outlet of the cooler; also ports are provided for measurement of static pressure at inlet and outlet ends of the cooler. A special arrangement is made in the block itself to facilitate the complete draining of oil present in the cooler at the end of the testing process.

The oil from the pump enters a specially designed manifold block (15). The block was designed so as to obtain different and constant oil flow rates. The flow control valves of constant flow type used were of two types namely, VSK2-G55 (16) and VSK2-G80 (17). The flow control valves were pre calibrated such that the G55 valve flow rate was set at 0.5 *lpm* and G80 valve flow rate was set to 1.5 *lpm*. In order to obtain different flow configurations flow outlet from the block was controlled by means of solenoid actuated (S01 - S05) poppet directional valves (18). 11 different flow configurations were achieved by operating the directional control valves in various combinations. The max. flow rate of 5.5 *lpm* was obtained by opening all the 5 directional control valves. When all the directional control valves are closed the flow is bypassed into the tank as shown in the circuit diagram.

When a pre-determined flow rate is selected, the flow enters the manifold block (13) on which the oil cooler is mounted. A pressure relief valve is provided for safety (14). In order to maintain leak proof joints between cooler inlet, cooler outlet and base block, a suitable fixture was designed so as to hold the cooler firmly on to the base block. The fixture is manually operated. An immersion oil heater (8) is provided in the tank to preheat the oil to a suitable temperature before the oil is passed into the cooler. The temperature of the oil in the tank is monitored using a PT100 type sensor connected to a temperature controller (7). The oil heater is connected to the temperature controller, it is switched on and off such that a set temperature is maintained. Temperature sensors (6) provided for oil temperature measurement are connected to DROs (7). Air exit temperature is measured via thermocouple connected to a DRO. The static pressure at oil inlet and outlet sides is measured using a pressure gauge. Arrangements are made such that

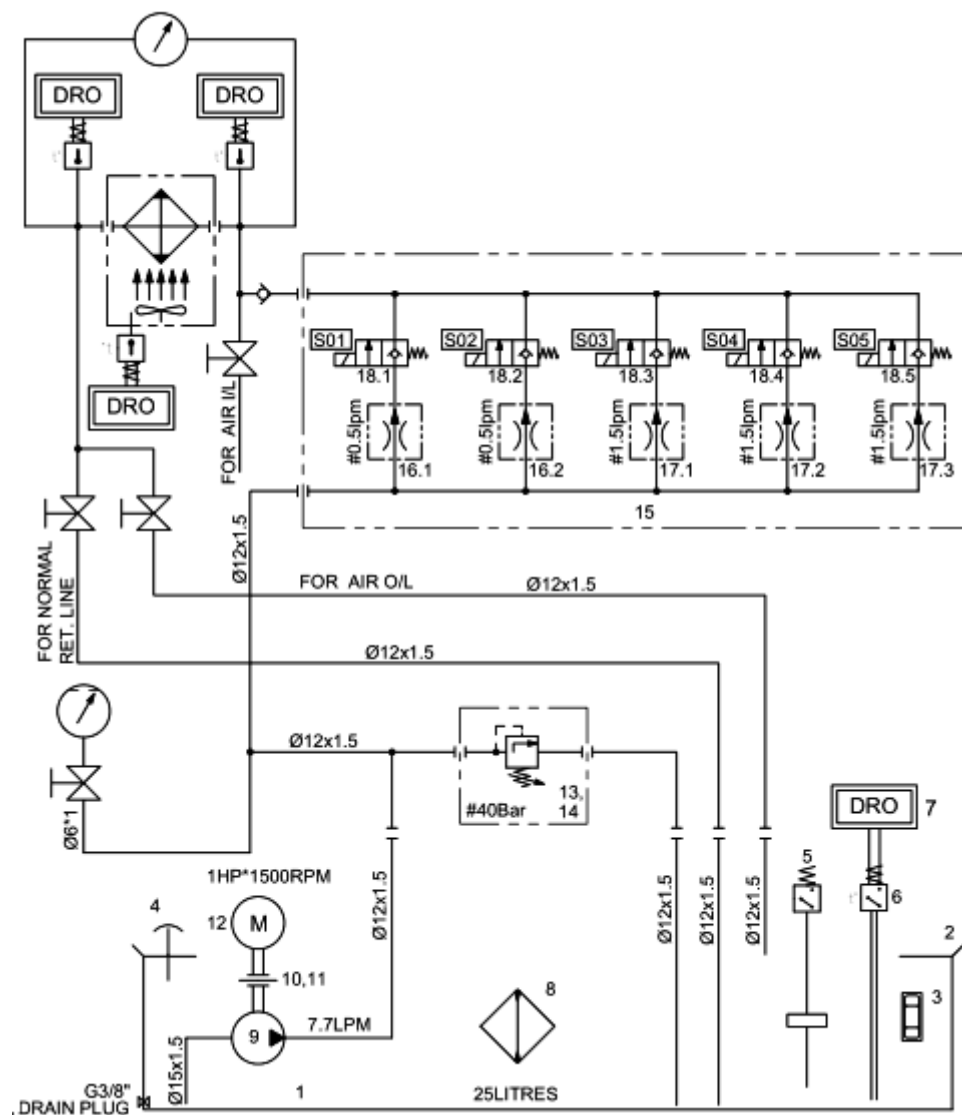


Figure 6. Testing arrangement

a differential pressure gauge can be employed.

4.0.1. Experimental observations The temperature readings for oil and air with specified oil flow rates were recorded. The flow rates chosen were 0.5 lpm, 1 lpm, 1.5 lpm, 2 lpm, 3 lpm and 5.5 lpm. A sample of readings taken is presented (Table 3).

4.0.2. Calculation of performance parameters from experimentally observed data A sample calculation is demonstrated for data corresponding to flow rate of 5.5 lpm and oil inlet temperature of 50 °C.

The geometric parameters like area are determined from respective equations used during theoretical thermo-hydraulic analysis. Here since all the temperatures; i.e. both oil inlet and oil

Table 3. Sample observations recorded from experiment (flow rate 3 lpm)

Oil flow rate	Oil inlet °C	Oil outlet °C	Air ambient °C	Air exit °C
3	46.9	42.0	30.0	35.0
	47.5	42.5	30.0	35.0
	47.8	42.8	30.0	36.0
	48.5	43.3	30.0	36.0
	49.2	43.9	30.0	37.0
	50.0	44.8	30.0	37.0
	50.5	44.5	30.0	37.0
	51.0	45.2	30.0	37.0
	51.5	45.5	30.0	37.0
	52.0	45.9	30.0	37.0

outlet, both air entry and exit temperatures are known, using an $\epsilon - NTU$ approach;

$$\begin{aligned}
 C_c = C_1 &= 97.00 \\
 C_h = C_2 &= 147.02 \\
 S_o, C_{min} &= C_1 \\
 \epsilon &= \frac{(T_{1,o} - T_{1,i})}{(T_{2,i} - T_{1,i})} \\
 \epsilon &= \frac{37 - 32}{50 - 32} = 0.2278 \\
 Q &= \epsilon C_{min} (T_{2,i} - T_{1,i}) \\
 &= 0.2778 * 97 * (50 - 32) = 485.0257 W
 \end{aligned}$$

5. Results and discussion

5.1. Effect of oil inlet temperature on exchanger effectiveness

The variation of heat exchanger effectiveness with oil inlet temperature is presented for an oil flow rate of 3 lpm (**Figure 7**). It can be observed that the actual effectiveness at any given oil inlet temperature is lower by around 12%. The reason for lower actual effectiveness may be attributed to the presence of various losses which were neglected during theoretical analysis. The actual experimental values are compared with values obtained using Manglik and Bergles correlation [4].

5.2. Effect of oil inlet temperature on heat transfer rate

The variation presented corresponds to an oil flow rate of 3 lpm (**Figure 8**). It can be observed that, both theoretical and actual curves follow an increasing trend with increasing oil inlet temperature while other parameters remain constant. The actual or experimental heat transfer rate values are around 13-15% lower compared to theoretically predicted results using Manglik and Bergles correlation [4]. The heat losses from oil tank, manifold blocks, various mechanical valves, cooler core geometric imperfections etc. lead to lower actual heat transfer rates, which were neglected during theoretical analysis.

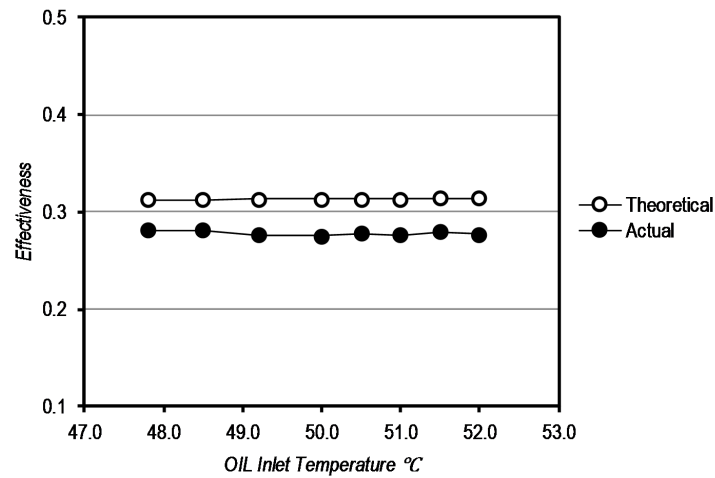


Figure 7. Plot of effectiveness vs oil inlet temperature

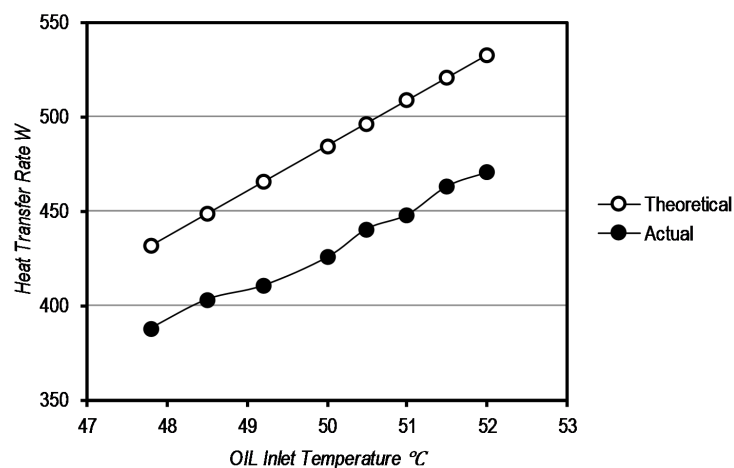


Figure 8. Plot of heat transfer rate vs oil inlet temperature

5.3. Effect of oil flow rate on effectiveness

The values of effectiveness were obtained at an oil inlet temperature of 50°C and air inlet temperature of 30°C (**Figure 9**). Both actual and theoretical curves almost coincide and represent a same trend, leading to the conclusion that an increase in oil flow rate decreases cooler effectiveness when other parameters are maintained constant.

5.4. Effect of oil flow rate on heat transfer rate

The values of heat transfer rate were obtained at an oil inlet temperature of 50°C and air inlet temperature of 30°C for different oil flow rates (**Figure 10**). The actual theoretical curves show an increase in heat transfer rate with increasing flow rates. This is due to increasing heat transfer coefficient owing to increasing Reynolds number and other associated parameters on the oil side of the cooler.

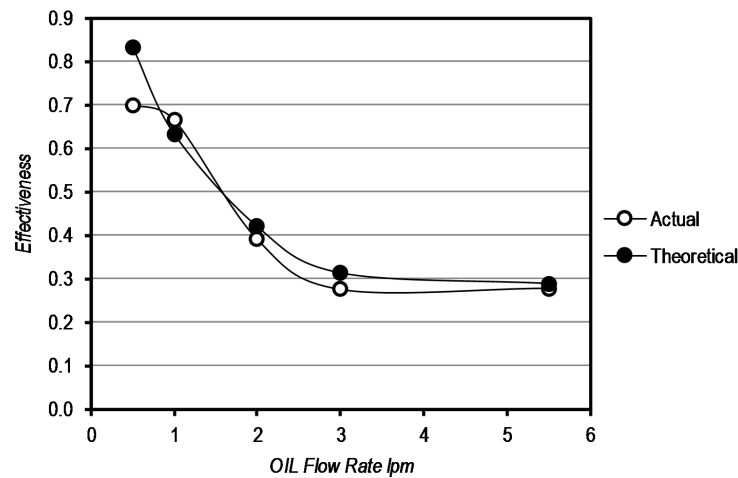


Figure 9. Plot of effectiveness vs oil flow rate

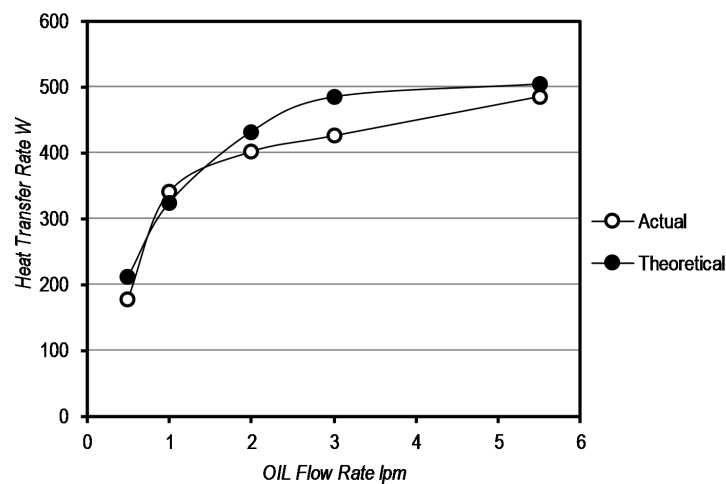


Figure 10. Plot of heat transfer rate vs oil flow rate

5.5. Pressure drop on oil side

The static pressure values were checked both at inlet and outlet sides of the cooler. It was found the pressure drop was below 2 kPa as predicted by theoretical pressure drop analysis for the maximum oil flow rate of 5.5 lpm . Since the flow rates in the return line of variable displacement pumps are typically below 3 lpm , it is concluded that the pressure drop is not appreciable enough to cause any hindrance and hence the pressure drop can be neglected.

5.6. Pressure drop on air side

Since the length of oil cooler core in the direction of air flow is only 32 mm , the pressure drop across the core was found to be negligible.

6. Conclusion

- The performance analysis of the air blast oil cooler was successfully accomplished. A test rig for the purpose was designed and developed. A detailed theoretical thermo-

hydraulic analysis of the cooler was performed prior to experimental investigation. The cooler effectiveness and heat transfer rate which were of prime interest were determined for various oil flow rate configurations and varying oil inlet temperatures.

- It was found that the cooler effectiveness varied only slightly with increasing oil inlet temperatures; whereas effectiveness decreased with increasing oil flow rates. In both the cases the experimental values were varied within 15% of theoretically predicted values.
- The heat transfer rate increased with increasing oil flow rates and also with increasing oil inlet temperatures. The main reason for the trend was found to be an increase in the value of heat transfer coefficient in both the cases. Even in this case, the experimental values obtained varied within 15% of theoretical results.
- The pressure drop for the oil side of the cooler was found negligible as both the experimental and theoretical results were well below the acceptable limit. The value of pressure drop for oil side did not exceed 0.05 bar even when maximum flow rate of 5.5 lpm was used. Also, for the air side the pressure drop was neglected due to core geometry and other parameters.

Acknowledgments

The authors wish to express gratitude towards Pascal Systemtechnik pvt. ltd., Bengaluru for the financial and technical support throughout the project. Also, thanks to BNMIT, Bengaluru for the support and encouragement.

References

- [1] Kays W M and London A L 1984 *Compact heat exchangers* 3rd ed. (New York: McGraw-Hill)
- [2] Joshi H M and Webb R L 1987 Heat transfer and friction in offset strip fin heat exchanger *Int. J. Heat and Mass Transfer* **30(1)** 69-84
- [3] Weiting A R Empirical correlation for heat transfer and flow friction characteristics of rectangular offset-fin plate-fin heat exchangers 1975 *J. of Heat Transfer* **97(3)** 488-490
- [4] Manglik R M and Bergles A E Heat transfer and pressure drop correlations for the rectangular offset strip fin compact heat exchanger 1995 *Experimental Thermal and Fluid Science* **10(2)** 171-180
- [5] Michna G J, Jacobi A M and Burton R L 2005 *Proc. Int. Conf. on Enhanced, Compact and Ultra-Compact Heat Exchangers: Science, Engineering and Technology (New Jersey)* vol 5 CHE2005-02
- [6] Mochizuki S and Yagi Transport Phenomena in stacks of interrupt parallel-plate surface 1987 *Exp. Heat Transfer* **109(1)** 127-140
- [7] Ganapathy V 1982 *Applied heat transfer* (Tulsa,OK: PennWell Books)

Nomenclature

A	total heat transfer surface area (both primary and secondary, if any)
A_o	minimum free-flow (or open) area on one fluid side of an exchanger
A_p	primary surface area on one side of an exchanger
b	distance between two plates in a plate-fin heat exchanger
C	flow stream heat capacity rate
C^*	heat capacity rate ratio
C_D	drag coefficient
c_p	specific heat at constant pressure
D_h	hydraulic diameter of flow passages
f	Fanning friction factor
G	fluid mass velocity based on the minimum free area
g_e	proportionality constant in Newton's second law of motion
h	heat transfer coefficient

k	fluid thermal conductivity for fluid
k_f	thermal conductivity of the fin material
k_w	thermal conductivity of the matrix (wall) material
L	fluid flow (core) length on one side of an exchanger
l_f	fin flow length on one side of a heat exchanger
l_s	strip length of an offset strip fin
m	fin parameter
\dot{m}	fluid mass flow rate
N_p	number of fluid passages
NTU	number of exchanger heat transfer units
Nu	Nusselt number
n_f	total number of fins on one fluid side of an extended-surface exchanger
Δp	fluid static pressure drop
q	total or local (whatever appropriate) heat transfer rate in an exchanger
r_h	hydraulic radius
V	heat exchanger total volume
Re	Reynolds number based on the hydraulic diameter
Pr	Prandtl number
δ	fin thickness
δ_w	wall thickness
ϵ	heat exchanger effectiveness
η_f	fin efficiency
η_o	extended surface efficiency on one fluid side of the extended surface heat exchanger
σ	ratio of free flow area to frontal area

Subscripts 1,2 indicate air and oil respectively when used.

Subscripts h, c indicate hot and cold respectively when used.